Introduction of a muscular bidirectional electrical anisotropy index to quantify the structural modifications during aging in raw meat

Introduction of a muscular bidirectional electrical anisotropy index to quantify the structural modifications during aging in raw meat

J A Gómez-Sánchez[1]**, W Aristizábal-Botero**[2]**, P J Barragán-Arango**[3] **and C J Felice**[1]

[1] Laboratorio de Medios e Interfases, DBI-INSIBIO/UNT-CONICET, CC 327, Tucumán 4000, Argentina
[2] Laboratorio de Instrumentación Biofísica, Departamento de Física, Universidad de Caldas, Manizales, Colombia
[3] Unidad Tecnológica de Alimentos, Universidad de Caldas, Calle 65 No. 26-10, Manizales, Colombia

E-mail: jgomez@herrera.unt.edu.ar

Abstract

In this paper, we propose an index (inherent electrical anisotropy: IEA) to quantify the changes of the electrical properties of bovine muscles during the aging process. The changes were measured by electrical impedance spectroscopy using tetrapolar electrode configuration. Our results are obtained for the tensor analysis of impedance measurements in muscle's samples along the longitudinal and transverse directions. This index improves several descriptions of the muscular anisotropy previously proposed by some authors about the degradation of the muscle due to the aging process. The index and IEA angle showed frequency dependence for each muscle with a significant decrement until the third day; thereafter the variations were smaller in the whole frequency range. This diminution is faster during the first storage days in the Longissimus Dorsi muscle compared with Biceps Brachii and Semi Membranous. The IEA suggests the tendency of each muscle to be homogenized. Based on results, it can be inferred that the index is a good indicator to monitor the structural changes that occur during aging; moreover, this index can also be employed to describe the anisotropy of different biological tissues and chemical compounds such as peptides and proteins.

(Some figures in this article are in colour only in the electronic version)

1. Introduction

The quality parameters of meat are grouped according to its organoleptic, nutritional and sanitary conditions (Geay *et al* 2001). Each of these parameters contributes in a larger or smaller degree to acceptability (Maltin *et al* 2003). The color, fat content, smell, firmness, tenderness, juiciness and flavor are the main characteristics in time on the basis of which the final consumer selects high-quality meat (Brackebusch *et al* 1991, Wulf and Page 2000). During storage, the action

of one or more systems of proteases is responsible for the post-mortem degradation of skeletal muscles. The proteolysis in fresh meat concerns several myofibrillar proteins; among them are titin, nebulin, desmin and troponin-T. This is partly due to the action of calpains and certain lysosomal enzymes as cathepsins (Uytterhaegen *et al* 1994, O'Halloran *et al* 1997, Mullen *et al* 2000). The calpain is responsible for the ruptures of the interactions between the Z-disk and the thin filament, the inter-myofibril links and the destruction of costameres during the aging process (Taylor *et al* 1995). Myofibril degradation

in the first days coincides with the reduction of the calpain activity and mechanical resistance in the muscle (Zamora *et al* 1996). During the muscle degradation process, the diameter of muscular cells decreases probably as a result of a contraction due to a reduction of the available space for the water molecules in the myofibril (Huff-Lonergan and Lonergan 2005). When the apoptosis process begins, an inversion of the phospholipid distribution occurs inside the cells, and the acidic components are replaced by others of basic nature (Herrera-Mendez *et al* 2006).

The structural properties of meat have been measured by using different techniques. During the aging process, these properties can be quantified through anisotropy measurements by using electrical impedance spectroscopy (EIS) (Lepetit *et al* 2002). EIS is a technique that measures small electric signals obtained as lineal response to the application of a sine wave current or voltage by employing electrodes within a frequency range (MacDonald 1992). These techniques have been used to measure the fat content by using insertion bipolar and tetrapolar electrodes as well as other configurations (Slanger and Marchello 1994, Marchello *et al* 1999, Velazco *et al* 1999, Whitman *et al* 1996, Lepetit *et al* 2002, Bohuslávek and Augustini 2003).

The measurements of electrical properties using bipolar electrodes exhibit a pseudo-capacitive phenomenon that depends on the frequency and the type of tissue. At low frequencies, the metallic electrodes produce a polarization effect on the surface of the electrode and the sample (Grosse and Tirado 2002). The tetrapolar technique, used initially by Geddes (1996), diminishes this polarization of electrodes at low frequency (Schwan and Ferris 1968). This is based on a couple of measurement electrodes with equal contact area (Prodan *et al* 2004). However, the tetrapolar systems are not exempted from the errors caused by the polarization resistance, because they can show another class of phenomena (Grimnes and Martinsen 2007).

The electric impedance measurements are modified by the direction, elongation and contraction of the muscular fibers (Swatland 1997). These measurements, carried out in both the parallel and transverse directions of the muscle fiber axis, show more significant variations in a frequency range of 10 kHz to 10 MHz called beta dispersion; these variations are mainly due to the Maxwell–Wagner effect (Gabriel *et al* 1996). The beta dispersion is caused by the ionic load in the capacitance of a cellular plasma membrane under the influence of an external electric field (Davey *et al* 1992). This dispersion depends on the tissue's structure, cell size, ionic state of the intra- and extracellular media and the membrane thickness (Dewberry 2000).

Measurements of electric properties are used to monitor the integrity of muscle membranes and gradual rupture of structures in the tissue (Bodakian and Hart 1994). Basic knowledge of the aging process allows an optimization of the storage times and this generates savings because some meat cuts can be matured in a few days, whereas other cuts take some weeks (Damez *et al* 2008). Byrne *et al* (2000) showed that the electric impedance measurements have a moderate correlation with meat quality characteristics. In other tests, Niu and

Lee (2000) observed that the maximum value of the phase angle changes during the storage time. The electric properties of the muscle change post-mortem and can describe the state of the muscle (Martinsen *et al* 2000). The contour of the muscular fibers of animals recently killed is not easily differentiable. After a day of storage, the fibers are characterized by a better contour definition; more storage time can cause the disintegration of the connective tissue (Bratzler 1971).

Several papers explain the aging process using measurements of electrical properties; these include a parameter and some indexes. Pliquett introduces the Py parameter as an indicator of the membrane integrity (Pliquett *et al* 2003). This is expressed by a percentage of variation of impedance measurements at low and high frequencies; these measurements have been made with insertion needle electrodes. On the other hand, Lepetit *et al* (2002) described an index that measures the electrical impedance at low and high frequencies along the longitudinal and transverse directions, and it depends on the post-mortem muscle degradation and can be quantized as an anisotropy quotient that relates the longitudinal and transverse measures. Damez *et al* (2008) established a lineal anisotropy index as the difference of the electric impedance measurements along the transverse and longitudinal direction. However, these indexes and this parameter have never used the capacitive properties of muscle membranes to quantify the anisotropy and the phase angle of electric impedance measurements. An additional disadvantage is that the electrodes used in these studies do not reduce the effects of the electrode electrolyte interface.

The objective of this paper is to propose an index of muscular bidirectional electrical anisotropy (inherent electrical anisotropy: IEA). This was compared with EIS measurements during the aging process of three bovine muscles in a frequency range between 2 kHz and 1.6 MHz. EIS measurements were carried out along the longitudinal and transverse directions to the muscular fibers. The electric parameters expressed by this index explain the structural variations of the muscular fibers and membranes in the degradation process during aging. A superficial tetrapolar adjacent probe was employed to decrease the electrode electrolyte interface (Felice and Valentinuzzi 1999) and can prevent the variability due to the insertion depth (Tsai *et al* 2000). We find that the IEA index serves as an indicator during the aging process of bovine muscles, and it presents a progressive decrement during the storage time and shows a tendency of each muscle to homogenize itself. The index IEA improves the mathematical description of the decrement of electrical anisotropy during the aging process; this theoretical analysis permits us to find the relationship among the integrity of muscular membrane, electrolytes released and the storage time.

2. Materials and methods

2.1. Index of muscular bidirectional electrical anisotropy (IEA)

The anisotropy is a quantitative parameter that shows the change of a physical characteristic due to the directional
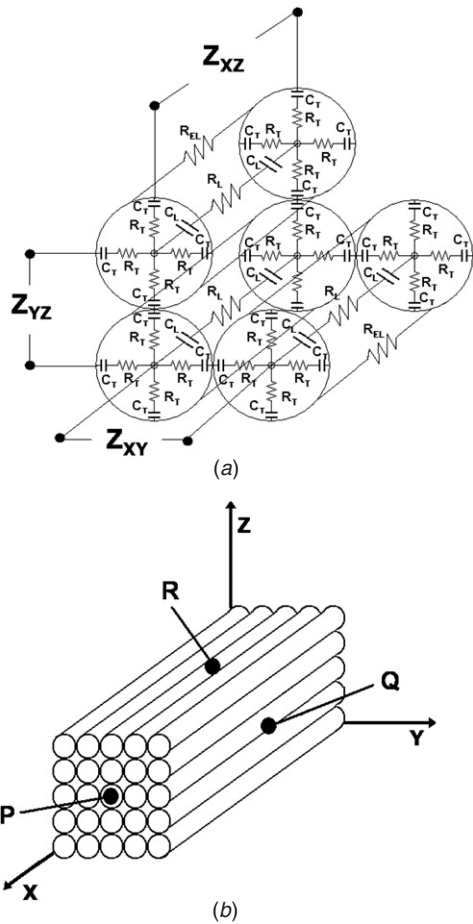
Figure 1. (*a*) Electrical model of muscle described using capacitances and resistances along the longitudinal and transverse directions, R_L: longitudinal resistance along the myofibril axis, R_T: transverse resistance (radial direction), R_{EL}: exterior resistance, C_L: longitudinal capacitance along the myofibril axis, C_T: transverse capacitance of membrane and connective tissue (radial direction). (*b*) Measurements of electrical impedance in each plane of muscle (point P: contact plane *YZ*, point *Q*: contact plane *XZ*, point R: contact plane *XY*).

variation. An electric anisotropy index of biological tissues must describe the resistive properties of intra- and extracellular media and pseudo-capacitive properties of membranes and connective tissue in both directions (longitudinal and transverse).

A myofibril is considered a tubular structure with a single anisotropy axis, frequently with a radial symmetrical distribution of this axis (Cruz-Orive *et al* 1985). The electrical properties of a myofibril can be described by using an isotropic cylinder of longitude *L* in the *X*-axis direction and radial *r* in the *Y*- and *Z*-axis directions (figure 1(*a*)).

The structure of muscle can be modeled by an electrical impedance tensor to characterize the total impedance of the system (Kun and Peura 1993). The electrical impedance of the muscle depends on the plane of contact on which the measurement electrode was placed (*P*, *Q* and *R*) as shown in figure 1(*b*), and it can be described by the components in each direction of the Cartesian axes *X*, *Y* and *Z* (figure 2). Depending on the complexity of the electrode geometry, there must be a
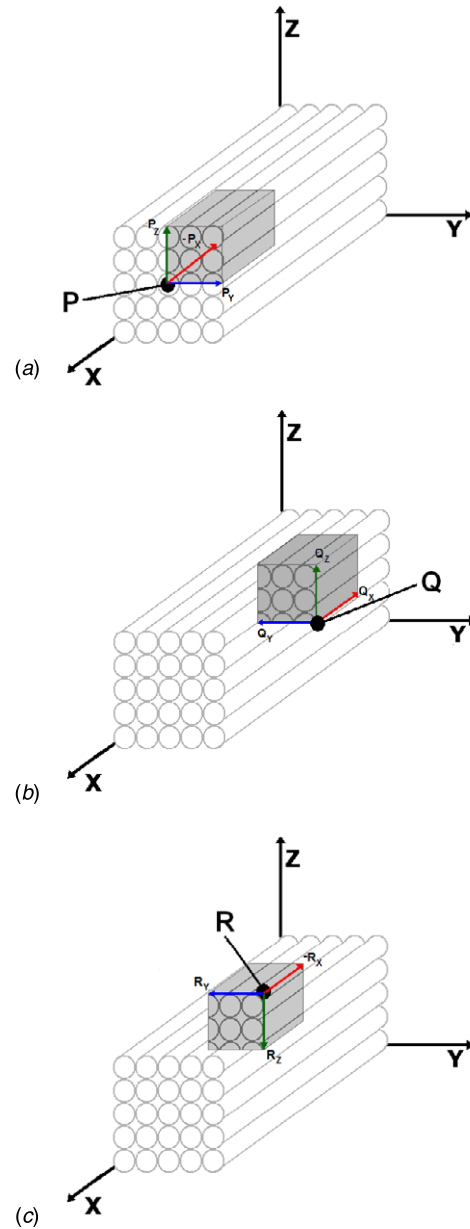

Figure 2. Schematic of the 3D Cartesian components of impedance measurements in each contact plane: (*a*) contact plane *YZ*, (*b*) contact plane *XZ* and (*c*) contact plane *XY*.

constant due to the depth of the excitation lines of the electric field applied on the tissue (K_{PR}), and also, there is another constant due to the area that was covered by the same field line on the measurement plane of the electrode (K_S). Based on the last description, equations (1)–(3) calculate the components *X*, *Y* and *Z* of electrical impedance to the contact planes *P*, *Q* and *R* respectively.

$$P_x = K_{PR}(R_L + jX_L) \qquad P_y = K_S(R_T + jX_T)$$
$$P_z = K_S(R_T + jX_T), \tag{1}$$

$$Q_x = K_S(R_L + jX_L) \qquad Q_y = K_{PR}(R_T + jX_T)$$
$$Q_z = K_S(R_T + jX_T), \tag{2}$$

$$R_x = K_S(R_L + jX_L) \qquad R_y = K_S(R_T + jX_T)$$
$$R_z = K_S(R_{PR} + jX_T). \tag{3}$$

There, the volumetric impedance of each contact plane (P, Q and R) can be represented by the vector sum of the contributions in each coordinate axis (equations (4)–(6)):

$$\vec{Z}_P = K_{PR}(R_L + jX_L)\hat{i} + K_S(R_T + jX_T)\hat{j}$$
$$+ K_S(R_T + jX_T)\hat{k}, \tag{4}$$

$$\vec{Z}_Q = K_S(R_L + jX_L)\hat{i} + K_{PR}(R_T + jX_T)\hat{j}$$
$$+ K_S(R_T + jX_T)\hat{k}, \tag{5}$$

$$\vec{Z}_R = K_S(R_L + jX_L)\hat{i} + K_S(R_T + jX_T)\hat{j}$$
$$+ K_{PR}(R_T + jX_T)\hat{k}. \tag{6}$$

The volumetric electrical impedance in each measurement plane can be described by a phasor in both magnitude and phase. The phasor magnitude is the value of the vector sum of the components in the three coordinated axes (equations (7a), (8a) and (9a)), and the phasor phase is the algebraic sum of each angle with respect to the two axes of the measurement plane (equations (7b), (8b) and (9b)).

Plane *YZ*:

$$|\vec{Z}_P| = \sqrt{[K_{PR}(R_L + jX_L)]^2 + 2K_S^2[(R_T + jX_T)]^2}, \tag{7a}$$

$$\theta_y = \tan^{-1}\left[\frac{K_S(R_T + jX_T)}{K_{PR}(R_L + jX_L)}\right];$$

$$\theta_z = \tan^{-1}\left[\frac{K_S(R_T + jX_T)}{K_{PR}(R_L + jX_L)}\right]. \tag{7b}$$

Plane *XZ*:

$$|\vec{Z}_Q| = \sqrt{[K_S(R_L + jX_L)] + \left(K_S^2 + K_{PR}^2\right)(R_T + jX_T)^2}, \tag{8a}$$

$$\theta_x = \tan^{-1}\left[\frac{K_S(R_L + jX_L)}{K_{PR}(R_T + jX_T)}\right];$$

$$\theta_z = \tan^{-1}\left[\frac{K_S(R_T + jX_T)}{K_{PR}(R_T + jX_T)}\right]. \tag{8b}$$

Plane *XY*:

$$|\vec{Z}_R| = \sqrt{[K_S(R_L + jX_L)] + \left(K_S^2 + K_{PR}^2\right)(R_T + jX_T)^2}, \tag{9a}$$

$$\theta_x = \tan^{-1}\left[\frac{K_S(R_L + jX_L)}{K_{PR}(R_T + jX_T)}\right];$$

$$\theta_y = \tan^{-1}\left[\frac{K_S(R_T + jX_T)}{K_{PR}(R_T + jX_T)}\right]. \tag{9b}$$

Now, we observe each muscle as a non-homogeneous and uniaxial medium; therefore, due to the geometry, various simplifications can be accomplished. Z_L was defined as the electrical impedance in the myofibril axis direction and Z_T as the electrical impedance in the transverse myofibril axis direction. Equation (10) shows the simplification for
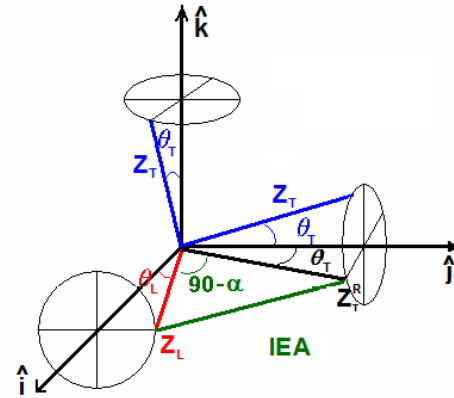

Figure 3. 3D phasors of impedance measurements in muscles.

a non-homogeneous system, and equation (11) for a uniaxial medium:

$$\vec{Z}_L \neq \vec{Z}_T, \tag{10}$$

$$\vec{Z}_P = \vec{Z}_L, \qquad \vec{Z}_Q = \vec{Z}_R = \vec{Z}_T. \tag{11}$$

Based on equations (10) and (11), the total impedance is expressed as a diagonal 3×3 tensor by using each element in the space coordinates (equation (12)):

$$Z = \begin{bmatrix} \vec{Z}_L & 0 & 0 \\ 0 & \vec{Z}_T & 0 \\ 0 & 0 & \vec{Z}_T \end{bmatrix}. \tag{12}$$

Again, the electrical impedance is given by a phasor expression as modulus and phase angle along the longitudinal (Z_L) and transverse directions (Z_T), see equations (13) and (14):

$$\vec{Z}_L = |Z_L|\langle\theta_L\rangle = |Z_L|\cos(\theta_L) + j|Z_L|\sin(\theta_L), \tag{13}$$
$$\vec{Z}_T = |Z_T|\langle\theta_T\rangle = |Z_T|\cos(\theta_T) + j|Z_T|\sin(\theta_T). \tag{14}$$

Based on equations (12)–(14), the electrical impedance is drawn on each plane and shown as three phasor elements in a tensor space on the Cartesian coordinates (figure 3).

Figure 3 shows that the transverse components have the same angle between the measurement axes. Therefore, it is possible to rotate the transverse electrical impedance Z_T on the planes (**i**, **k**) and (**j**, **k**) to the plane (**i**, **j**). This rotation vector is on the same plane of the longitudinal component; the segment line between the longitudinal and transverse components represents the muscular bidirectional electrical impedance, and now we call this IEA; the index was found by using the Al-Kashi theorem or the generalized cosine law (equation (15)), an extended version of Pythagorean theorem:

$$IEA = (\sqrt{|Z_L|^2 + |Z_T|^2 - 2|Z_L||Z_T|\cos(90 - \alpha)}) \tag{15}$$

The alpha angle or the IEA angle can be calculated as the sum of the phase angles from equation (16):

$$\alpha = \theta_T + \theta_L. \tag{16}$$

In equation (12), Z_L and Z_T are the magnitude of the electrical impedance measurement along the longitudinal and transverse

Figure 4. Electrical impedance spectroscopy MK3.5 single channel system.

directions respectively, and the alpha angle is the sum of the longitudinal and transverse phase angles.

The myofibril geometry is the implicit IEA index; this allows us to determine the muscular degradation process during the storage time.

2.2. Muscle samples preparation

First, we select randomly a Brahman–Zebu cross cattle (weight: 470 kg, age: 36 months) of a commercial meat processing plant (Frigocentro, Manizales). After the slaughter, the carcass has been disposed for 2 h in a chilled room; later the meat was stored in a cold camera room for 24 h at 4 °C. The following step was taken to extract the three muscles (LD: Longissimus Dorsi, BB: Biceps Brachii and SM: Semi Membranous) of low, medium and high toughness, in accordance with the Belew WBS data (Belew *et al* 2003).

Muscles were stored in a portable refrigerator and taken to the Unidad Tecnológica de Alimentos at the Universidad de Caldas. Each muscle was cut along the transverse direction of myofibrils in order to extract 1.8 cm wide, 1.8 cm high and 2.6 cm long pieces.

The pieces of each muscle were packed in a polypropylene and nylon bag (70 μm thick) using the Plusvac 20 system (KOMET GmbH). Each individual bag contains six samples, two of each muscle. We packed 14 bags for the daily tests and store them at 4 °C. The room temperature during the experiments was 20 °C. Muscle pH was monitored using a pH meter Toledo MP220 with auto calibration by temperature. The electrode of the pH meter was inserted approximately in the middle of each sample of the muscle.

2.3. Electrical impedance spectroscopy measurements

Electrical impedance spectroscopy (EIS) measurements were carried out by using an EIS MK3.5 single-channel system (figure 4). This device was designed and constructed in the

Department of Medical Physics and Clinical Engineering, University of Sheffield, UK. This device is both a signal generator and a measurement instrument, and it must be connected by a USB port of an IBM compatible computer. The electrical impedance measurements are carried out with a constant sinusoidal current of 20 μA. This current is applied between a pair of electrodes in a frequency range between 2 kHz and 1.6 MHz. A computer screen displays the impedance data value in real time by using software developed in Matlab (Wilson *et al* 2001).

The probe has a pen shape with four gold electrodes of 1 mm diameter such as described by Brown *et al* (2000). This equipment was calibrated by the manufacturer by using identical probes. The manufacturer advises recalibrating this device by means of a saline solution of 10 Ω m resistivity.

2.4. Experimental protocols

The first measurements were carried out 30 h after slaughtering and on the following days: 2, 3, 4, 7, 9, 10, 11, 12 and 14. Every day, an individual bag was taken from the refrigerator, each closed package was deposited inside a container of water at 20 °C for an hour and subsequently the bag was extracted from the container. The pieces of meat were removed from the bag and thereafter placed into an acrylic box to avoid contact of the tissue with conductive metallic surfaces. This procedure impedes drastic temperature changes and prevents rare impedance variations due to the temperature; the operator needs to use latex gloves to inhibit sample contamination. Both room and sample temperatures were 20 ± 1 °C during the experiments.

The variability of measurements due to the pressure of the electrode on the sample was prevented by means of a single operator. We carried out the magnitude and phase measurements of electrical impedance in each piece along the longitudinal and transverse directions of the myofibril's axis at three points: central, right and left, and each of these measurements was repeated twice to observe the reproducibility.

The values obtained by EIS measurements have been analyzed using a Cartesian axis 3D draw with MATLAB®. This graph shows the storage time on the *X* Cartesian axis, the applied frequency on the *Y* Cartesian axis and the value of the module and the IEA angle on the *Z* Cartesian axis.

3. Results

Based on equation (15) we solve the IEA index for the three muscles at each frequency. Figure 5 shows the frequency dependence of each muscle with different behavior from the first day. The index value on day 1 was higher in the Longissimus Dorsi muscle (IEA 13.99) compared with the two other muscles (Biceps Brachii IEA = 7.51, Semi Membranous IEA = 4.27). Additionally, the difference of IEA between low and high frequency (ΔIEA) was greater in Longissimus Dorsi (ΔIEA = 12.91) than the other muscles (Biceps Brachii ΔIEA = 7.20, Semi Membranous ΔIEA = 2.65).
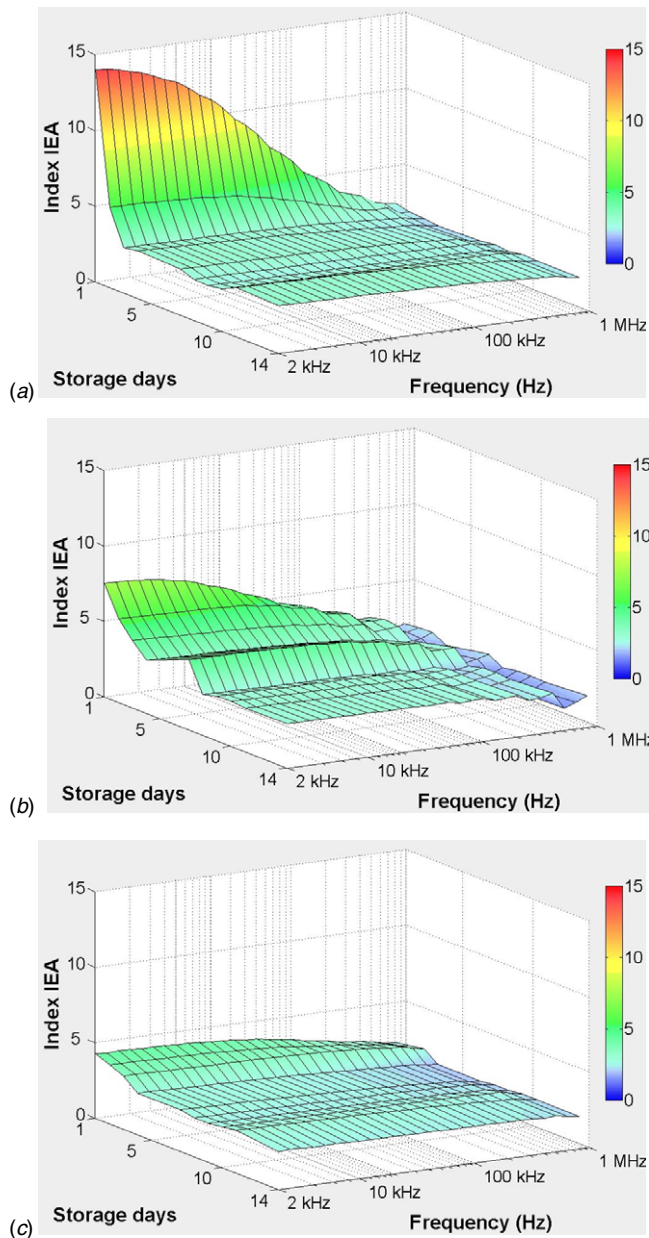
Figure 5. IEA index of each muscle: (*a*) Longissimus Dorsi, (*b*) Biceps Brachii and (*c*) Semi Membranous. A color bar indicates the magnitude of the IEA index in 3D graphs. IEA index decreases more quickly during the first storage days in the Longissimus Dorsi muscle compared with Biceps Brachii and Semi Membranous.

Figure 6. IEA angle of each muscle: (*a*) Longissimus Dorsi, (*b*) Biceps Brachii and (*c*) Semi Membranous. The figure axes are storage days (1–14), frequency (2 kHz–1.6 MHz) and angle α (0–75°). A color bar indicates the magnitude of the index in 3D graphs.

The IEA shows a significant decrement during the first three days of the storage time in the three muscles at each applied frequency. The decrement at 2 kHz is minor in the Biceps Brachii (86.42%) and Semi Membranous (87.24%) muscles compared with the Longissimus Dorsi muscle (95.84%), whereas at 1.6 MHz the decrement was superior to 97% in all muscles. After 4 days, the variations of IEA were smaller in the whole frequency range for all muscles (Longissimus Dorsi < 5%, Biceps Brachii < 10%, Semi Membranous < 10%).

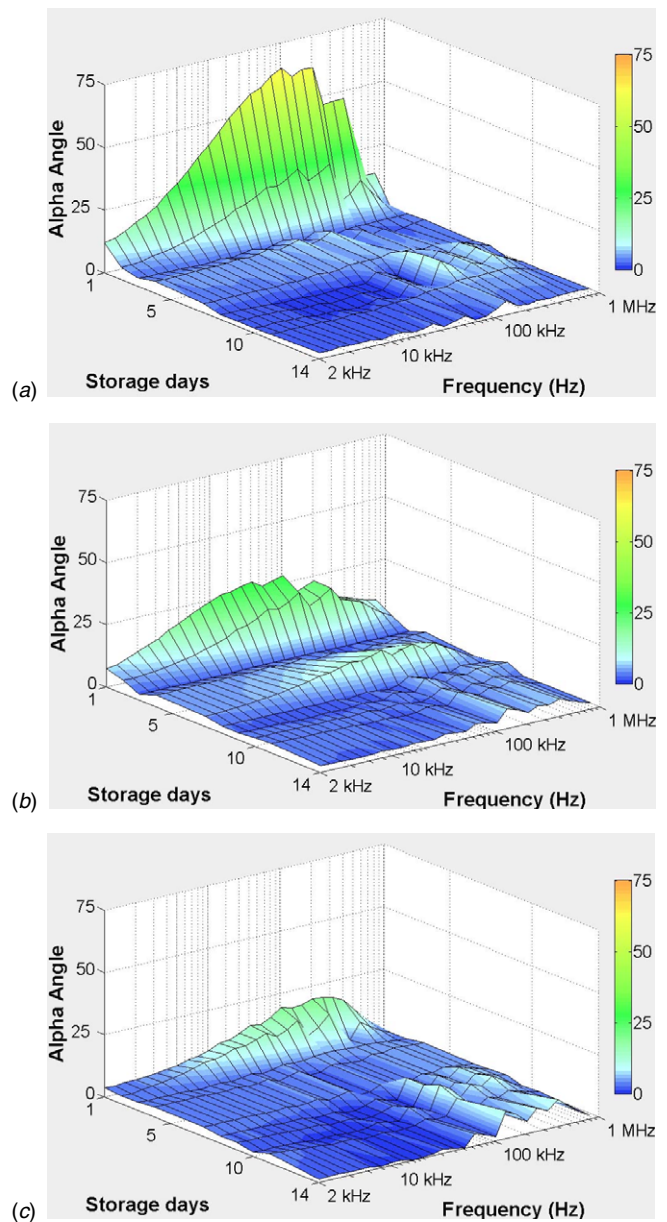The values of the IEA angle were calculated for all muscles as from equation (16) and each respective graph is shown in figure 6. The IEA angle depends on the applied frequency: a maximum value was seen on the first day; the highest IEA angle is seen in the Longissimus Dorsi muscle ($\alpha = 65.02$) and lower in the Biceps Brachii ($\alpha = 28.57$) and Semi Membranous ($\alpha = 16.64$) muscles. The IEA angle decreases during the storage time, the maximum decrease appears in the first three days in Longissimus Dorsi (96.25%), Semi Membranous (93.86%) and Biceps Brachii (73.63%). After the third day, the IEA index has dissimilar behavior for all muscles; at frequencies <100 kHz the IEA angle reaches a steady state but at frequencies >100 kHz unstable behavior occurs.

Table 1. Bidirectional muscular electrical anisotropy index (IEA) values throughout the storage time.

| Muscle | Day | $F_1 = 2$ kHz | | $F_1 = 100$ kHz | | $F_1 = 1.6$ MHz | | Frequency α_{max} |
		Index	Angle	Index	Angle	Index	Angle	
Longissimus Dorsi	1	13.6 ± 2.33	12.2 ± 0.04	6.2 ± 1.12	65.0 ± 0.11	1.6 ± 0.43	14.1 ± 0.02	101.6 kHz
	2	5.3 ± 0.54	5.0 ± 0.01	3.9 ± 0.24	27.5 ± 0.02	1.5 ± 0.16	3.0 ± 0.007	101.6 kHz
	3	3.0 ± 0.16	3.3 ± 0.01	2.8 ± 0.13	5.1 ± 0.01	1.5 ± 0.08	3.5 ± 0.01	101.6 kHz
	4	3.1 ± 0.23	4.6 ± 0.01	2.7 ± 0.18	7.8 ± 0.01	1.5 ± 0.11	3.7 ± 0.01	101.6 kHz
	7	3.0 ± 0.35	3.8 ± 0.01	2.8 ± 0.34	5.4 ± 0.01	1.4 ± 0.32	3.2 ± 0.01	128.0 kHz
	8	2.7 ± 0.20	2.0 ± 0.01	2.6 ± 0.23	0.5 ± 0.01	1.6 ± 0.21	4.0 ± 0.01	128.0 kHz
	9	2.7 ± 0.08	2.1 ± 0.01	2.6 ± 0.09	0.9 ± 0.01	1.5 ± 0.08	1.8 ± 0.01	128.0 kHz
	10	2.8 ± 0.29	2.0 ± 0.01	2.7 ± 0.29	1.1 ± 0.01	1.6 ± 0.26	2.9 ± 0.01	128.0 kHz
	11	3.2 ± 0.34	2.1 ± 0.01	2.9 ± 0.24	4.4 ± 0.01	1.6 ± 0.09	2.5 ± 0.01	306.4 kHz
	14	3.1 ± 0.26	2.6 ± 0.01	2.9 ± 0.22	3.3 ± 0.01	1.5 ± 0.15	2.8 ± 0.01	128.0 kHz
Biceps Brachii	1	7.5 ± 1.76	7.5 ± 0.05	4.3 ± 0.64	28.1 ± 0.07	2.2 ± 0.20	9.5 ± 0.01	50.8 kHz
	2	5.6 ± 1.40	5.3 ± 0.02	4.5 ± 0.68	24.0 ± 0.04	2.3 ± 0.29	5.6 ± 0.01	101.6 kHz
	3	4.5 ± 0.58	2.2 ± 0.01	3.8 ± 0.29	2.5 ± 0.02	2.3 ± 0.14	2.2 ± 0.01	101.6 kHz
	4	3.5 ± 0.31	4.8 ± 0.01	3.1 ± 0.22	4.9 ± 0.02	1.8 ± 0.23	4.5 ± 0.01	50.8 kHz
	7	4.6 ± 0.41	4.3 ± 0.01	4.1 ± 0.29	14.1 ± 0.01	2.3 ± 0.16	2.9 ± 0.01	101.6 kHz
	8	2.7 ± 0.17	2.8 ± 0.01	2.5 ± 0.17	2.6 ± 0.01	1.8 ± 0.15	3.4 ± 0.01	128.0 kHz
	9	2.9 ± 0.22	2.7 ± 0,01	2.8 ± 0.23	2.4 ± 0.01	1.9 ± 0.17	5.7 ± 0.01	128.0 kHz
	10	3.0 ± 0.08	3.3 ± 0.011	2.8 ± 0.09	3.1 ± 0.01	2.0 ± 0.08	2.6 ± 0.01	128.0 kHz
	11	2.9 ± 0.17	3.8 ± 0,01	2.7 ± 0.15	2.2 ± 0.01	1.9 ± 0.07	2.8 ± 0.01	128.0 kHz
	14	2.9 ± 0.10	2.8 ± 0.01	2.8 ± 0.12	3.3 ± 0.01	2.1 ± 0.10	2.8 ± 0.01	128.0 kHz
Semi Membranous	1	4.3 ± 0.28	3.7 ± 0.01	3.5 ± 0.23	19.4 ± 0.02	2.3 ± 0.07	3.7 ± 0.01	101.6 kHz
	2	3.9 ± 0.63	3.1 ± 0.01	3.4 ± 0.28	16.6 ± 0.02	2.5 ± 0.12	2.9 ± 0.01	101.6 kHz
	3	3.5 ± 0.09	3.2 ± 0.01	3.3 ± 0.10	5.0 ± 0.01	2.6 ± 0.10	3.1 ± 0.01	161.3 kHz
	4	2.7 ± 0.26	4.1 ± 0.01	2.4 ± 0.20	4.2 ± 0.01	2.0 ± 0.11	4.2 ± 0.01	406.4 kHz
	7	2.7 ± 0.20	4.0 ± 0.01	2.4 ± 0.20	4.2 ± 0.01	2.0 ± 0.11	3.9 ± 0.01	406.4 kHz
	8	2.6 ± 0.23	2.9 ± 0.01	2.4 ± 0.23	0.6 ± 0.01	2.1 ± 0.18	4.3 ± 0.01	128.0 kHz
	9	2.6 ± 0.23	2.9 ± 0.01	2.4 ± 0.23	0.6 ± 0.01	2.1 ± 0.18	4.5 ± 0.01	128.0 kHz
	10	2.7 ± 0.23	1.8 ± 0.01	2.6 ± 0.23	1.6 ± 0.01	2.2 ± 0.10	2.8 ± 0.01	128.0 kHz
	11	2.8 ± 0.15	3.9 ± 0.01	2.6 ± 0.17	2.1 ± 0.01	2.2 ± 0.14	3.2 ± 0.01	128.0 kHz
	14	2.5 ± 0.13	1.5 ± 0.01	2.6 ± 0.16	1.8 ± 0.01	2.1 ± 0.14	1.6 ± 0.01	128.0 kHz

Table 1 shows the index and IEA angle throughout the storage time. In the first two days, the index IEA at 2 kHz presents variability between 6.5% and 23.47%; the variation was higher in Biceps Brachii and less in Semi Membranous; the variability between samples decreased when the frequency was increased. The IEA module decreases more quickly in all muscles at 2 kHz in the first three days, moderately at 100 kHz and gradually at 1.6 MHz. The decrement of the IEA module was slow in the following days.

Otherwise, the IEA angle had a maximum value at a particular frequency (IEA frequency) on the first day. The maximum value of the IEA angle reduced during the storage time, whereas the IEA frequency increased up to a steady value for all muscles. The variability of the IEA angle is lower than 2%.

The average of pH measurements in the three muscles during the storage time was 5.62 (SD = 0.1).

4. Discussion

Several authors have carried out measurements of electrical properties in bovine muscles during the aging process along the longitudinal and transverse directions and they found a ratio of anisotropy, which decreases during the aging time (Lepetit *et al* 2002, Pliquett *et al* 2003, Damez *et al* 2008). These papers proposed parameters and indexes to calculate the anisotropy by using electrical measurements in muscles, but they did not include tensor studies of electrical properties to explain this behavior.

The electrical properties of muscles in animals recently slaughtered are highly anisotropic, but this anisotropy decreased during the storage time (Foster and Schwan 1989), which is reflected by a higher resistivity in the transverse direction compared with the longitudinal direction (Hart *et al* 1999). The IEA index shows this behavior from the first day of the aging process and a higher anisotropy at frequencies lower than 100 kHz; the progressive decrement of the IEA index during the storage time is dissimilar for all muscles, that is, due to the different structural conformation in each muscle, connective tissue and myofibril geometry (Passerieux *et al* 2006), many structural changes in the muscle occur in the longitudinal and transverse directions due to rupture and fragmentation of myofibrils (Tornberg 1996).

The gradual rupture of connective structures and membranes leads to the reduction of the tissue anisotropy (Bodakian and Hart 1994); this causes the liberation of electrolytes stored into sarcoplasm, and subsequently these blend with the extracellular medium in the whole muscle. The decrement of the IEA index is faster during the first three days and we infer, based on our results, that the quantity of

released electrolytes is higher during these days because the electrical impedance is diminished due to higher electrolyte concentration outside the myofibril (figure 5). This change is similar to the decrease of Py modulus (Pliquett *et al* 2003).

The sarcolem rupture produces a minor contribution to the membrane capacitance and consequently to the phase angle. This muscle degradation is presented by free ion diffusion between membranes which were previously impermeable and produces a progressive decrement in the IEA angle value, to reach a low value (figure 6). The sarcolems of the muscle disappear during storage time; it is caused by the degradation of sarcolems due to the aging process as reported by Niu and Lee (2000).

This paper shows that the index and IEA angle in each muscle differ, in other words, every muscle present a dissimilar degradation process due to their physiological parameters. They can be related to the longitude and diameter of muscle fibers and the dependence on endogenous and exogenous factors such as sex, age, muscle position, exercise and nutrition. The structure and quantity of connective tissue in the muscle generally depend more on the physical activity (Pearson 1990).

5. Conclusion

The mechanism responsible for muscular anisotropy is still a subject of study in terms of muscle physiology. According to our measurements carried out in aging meat, each muscle has a particular degradation level due to its structure and it determines a different anisotropy level of each individual muscle.

The IEA index and the previously proposed index help to study the muscular degradation. The index proposed here allows finding the progressive degradation of muscle sarcolems by using the longitudinal and transverse measurements of electrical impedance when the variations of index and angle IEA are calculated.

The quantification of the muscular bidirectional electric anisotropy index is a good indicator to determine the meat storage time and it can be used to predict its quality. This index also serves as an electric anisotropy indicator of chemical compounds and biological structures.

Acknowledgments

References

Belew J B, Brooks J C, McKenna D R and Savell J W 2003 Warner–Bratzler shear evaluations of 40 bovine muscles *Meat Sci.* **64** 507–12

Bodakian B and Hart F X 1994 The dielectric properties of the meat *IEEE Trans. Dielectr. Electr. Insul.* **1** 181–7

Bohuslávek Z and Augustini C H 2003 Prediction of commercial classification values of beef carcasses by means of the bioelectrical impedance analysis (BIA) *Czech J. Anim. Sci.* **48** 243–50

Brackebusch A, Carr T R, McKeith F K, Dutton D M and McLaren D G 1991 Relationship between marbling group and major muscle contribution to beef carcass mass *J. Anim. Sci.* **69** 625–30

Bratzler L J 1971 *The Science of Meat and Meat Products* ed J F Price and B S Schweigert (San Francisco: Freeman) p 512

Brown B H, Tidy J A, Boston K, Blackett A D, Smallwood R H and Sharp F 2000 Relation between tissue structure and imposed electrical current flow in cervical neoplasia *The Lancet* **355** 892–5

Byrne C E, Troy D J and Buckley D J 2000 Postmortem changes in muscle electrical properties of bovine M longissimus dorsi and their relationship to meat quality attributes and pH fall *Meat Sci.* **54** 23–34

Cruz-Orive L M, Hoppeler H, Mathieu O and Weibel E R 1985 Stereological analysis of anisotropic structures using directional statistics *Appl. Stat.* **34** 14–32

Damez J L, Clerjon S, Abouelkaram S and Lepetit J 2008 Beef meat electrical impedance spectroscopy and anisotropy sensing for non-invasive early assessment of meat aging *J. Food Eng.* **85** 116–22

Davey C L, Davey H M and Kell D B 1992 On the dielectric properties of cell suspensions at high volume fractions *Bioelectrochem. Bioenerg.* **28** 319–40

Dewberry B 2000 A review of electrical impedance spectrometry methods for parametric estimation of physiologic fluid volumes *MSFC Center Director's Discretionary Fund Final Report, Project No. 96-03* (AL, USA: Marshall Space Flight Center)

Feldman Y, Nigmatullin R, Polygalov E and Texter J Fractal-polarization correction in time domain dielectric spectroscopy *Phys. Rev.* E **58** 7561–5

Felice C J and Valentinuzzi M E 1999 Medium and interface components in impedance microbiology *IEEE Trans. Biomed. Eng.* **46** 1483–7

Foster K R and Schwan H P 1989 Dielectric properties of tissues and biological materials: a critical review *Crit. Rev. Biomed. Eng.* **17** 25–104

Gabriel S, Lau R W and Gabriel C 1996 The dielectric properties of biological tissues: II. Measurements in the frequency range 10 Hz to 20 GHz *Phys. Med. Biol.* **41** 2251–69

Geay Y, Bauchart D, Hocquette J F and Culioli J 2001 Effect of nutritional factors on biochemical, structural and metabolic characteristics of muscles in ruminants, consequences on dietetic value and sensorial qualities of meat *Reprod. Nutr. Dev.* **41** 1–26

Geddes L A 1996 Who introduced the tetrapolar method for measuring resistance and impedance? *IEEE Eng. Med. Biol. Mag.* **15** 133–4

Grimnes S and Martinsen O G 2007 Sources of error in tetrapolar impedance measurements on biomaterials and other ionic conductors *J. Phys. D: Appl. Phys* **40** 9–14

Grosse C and Tirado M C 2002 Low-frequency dielectric spectroscopy of colloidal suspensions *J. Non-Cryst. Solids* **305** 386–92

Hart F X, Berner N J and McMillen R L 1999 Modelling the anisotropic electrical properties of skeletal muscle *Phys. Med. Biol.* **44** 413–21

Herrera-Mendez C H, Becila S, Boudjellal A and Ouali A 2006 Meat aging: reconsideration of the current concept *Trends Food Sci. Technol.* **17** 394–405

Huff-Lonergan E and Lonergan S M 2005 Mechanisms of water-holding capacity of meat: the role of postmortem biochemical and structural changes *Meat Sci.* **71** 194–204

Kun S and Peura R A 1993 Model of anisotropic skeletal muscle resistivity behaviour *Proc. 15th Ann. Int. Conf. IEEE Engineering in Medicine and Biology Society (San Diego, CA, USA, 28–31 October 1993)* pp 1192–3

Lepetit J, Sale P, Favier R and Dalle R 2002 Electrical impedance and tenderisation in bovine meat *Meat Sci.* **60** 51–62

Macdonald J R 1992 Impedance spectroscopy *Ann. Biomed. Eng.* **20** 289–305

Maltin C, Balcerzak D, Tilley R and Delday M 2003 Determinants of meat quality: tenderness *Proc. Nutr. Soc.* **62** 337–47

Marchello M J, Slanger W D and Carlson J K 1999 Bioelectrical impedance: fat content of beef and pork from different size grinds *J. Anim. Sci.* **77** 2464–8

Martinsen E G, Grimnes S and Mirtaheri P 2000 Non-invasive measurements of post-mortem changes in dielectric properties of haddock muscle—a pilot study *J. Food Eng.* **43** 189–92

Mullen A M, Murray B and Troy D 2000 Predicting the eating quality of meat *Final Report Project Armis No. 4391* (Dublin, Ireland: TEAGASC Agriculture and Food Development Authority)

Niu J and Lee J Y 2000 A new approach for the determination of fish freshness by electrochemical impedance spectroscopy *J. Food Sci.* **65** 780–5

O'Halloran G R, Troy D J, Buckley D J and Reville W J 1997 The role of endogenous proteases in the tenderisation of fast glycolysing muscle *Meat Sci.* **47** 187–210

Passerieux E, Rossignol R, Chopard A, Carnino A, Marini J F, Letellier T and Delage J P 2006 Structural organization of the perimysium in bovine skeletal muscle: junctional plates and associated intracellular subdomains *J. Struct. Biol.* **154** 206–16

Pearson A M 1990 Muscle growth and exercise *Crit. Rev. Food Sci. Nutr.* **29** 167–96

Pliquett U, Altmann M, Pliquett F and Schöberlein L 2003 Py—a parameter for meat quality *Meat Sci.* **65** 1429–37

Prodan C, Mayo F, Claycomb J R and Miller J H Jr 2004 Low-frequency, low-field dielectric spectroscopy of living cell suspensions *J. Appl. Phys.* **95** 3754–6

Schwan H P and Ferris C D 1968 Four-electrode null techniques for impedance measurement with high resolution *Rev. Sci. Instrum.* **39** 481–5

Slanger W D and Marchello M J 1994 Bioelectrical impedance can predict skeletal muscle and fat-free skeletal muscle of beef cow primal cuts *J. Anim. Sci.* **72** 3124–30

Swatland H J 1997 Observations on rheological, electrical, and optical changes during rigor development in pork and beef *J. Anim. Sci.* **75** 975–85

Taylor R G, Geesink G H, Thompson V F, Koohmaraie M and Goll D E 1995 Is Z-disk degradation responsible for postmortem tenderization? *J. Anim. Sci.* **73** 1351–67

Tornberg E 1996 Biophysical aspects of meat tenderness *Meat Sci.* **43** S175–91

Tsai J Z, Cao H, Tungjitkusolmun S, Woo J E, Vorperian V R and Webster J G 2000 Dependence of apparent resistance of four-electrode probes on insertion depth *IEEE Trans. Biomed. Eng.* **47** 41–8

Uytterhaegen L, Claeys E and Demeyer D 1994 Effects of exogenous protease effectors on beef tenderness development and myofibrillar degradation and solubility *J. Anim. Sci.* **72** 1209–23

Velazco J, Morrill J R and Grunewald K K 1999 Utilization of bioelectrical impedance to predict carcass composition of Holstein steers at 3, 6, 9, and 12 months of age *J. Anim. Sci.* **77** 131–6

Whitman T A, Forrest J C, Morgan M T and Okos M R 1996 Electrical measurement for detecting early postmortem changes in porcine muscle *J. Anim. Sci.* **74** 80–90

Wilson A J, Milnes P, Waterworth A R, Smallwood R H and Brown B H 2001 Mk3.5: a modular, multi-frequency successor to the Mk3 a EIS/EIT system *Physiol. Meas.* **22** 49–54

Wulf D M and Page J K 2000 Using measurements of muscle color, pH, and electrical impedance to augment the current USDA beef quality grading standards and improve the accuracy and precision of sorting carcasses into palatability groups *J. Anim. Sci.* **78** 2595–607

Zamora F, Debiton E, Lepetit J, Lebert A, Dransfield E and Ouali A 1996 Predicting variability of aging and toughness in beef *M. Longissimus lumborum et thoracis Meat Sci.* **43** 321–33